

University of Groningen

The opacity of spiral galaxy disks.

Holwerda, Benne

IMPORTANT NOTE: You are advised to consult the publisher's version (publisher's PDF) if you wish to cite from it. Please check the document version below.

Document Version

Publisher's PDF, also known as Version of record

Publication date:

2005

[Link to publication in University of Groningen/UMCG research database](#)

Citation for published version (APA):

Holwerda, B. (2005). *The opacity of spiral galaxy disks*. s.n.

Copyright

Other than for strictly personal use, it is not permitted to download or to forward/distribute the text or part of it without the consent of the author(s) and/or copyright holder(s), unless the work is under an open content license (like Creative Commons).

The publication may also be distributed here under the terms of Article 25fa of the Dutch Copyright Act, indicated by the "Taverne" license. More information can be found on the University of Groningen website: <https://www.rug.nl/library/open-access/self-archiving-pure/taverne-amendment>.

Take-down policy

If you believe that this document breaches copyright please contact us providing details, and we will remove access to the work immediately and investigate your claim.

Downloaded from the University of Groningen/UMCG research database (Pure): <http://www.rug.nl/research/portal>. For technical reasons the number of authors shown on this cover page is limited to 10 maximum.

8

Future work with the Synthetic Field Method

Based on:

HST AT cycle-14 proposals 450 and 453, both accepted

Abstract

The installation of the Advanced Camera for Surveys in the Hubble Space Telescope in 2002, opened up the possibility of quickly imaging the whole of the disk of spiral galaxies. The ACS is a improvement in accuracy, resolution, field-of-view over the WFPC2 camera and several datasets are now in the archive, that could be used for similar analysis as done in the previous Chapters. The most notable and suitable ones are those on M51 and M101. This Chapter briefly highlights the possibilities of these data-sets to complement and improve on the work done with the WFPC2.

8.1 Justification for more SFM analysis

Dust in spiral disks not only alters our perception of spirals but is also an important catalyst and component of the interstellar matter, both chemically and dynamically. Recently, a cold component ($T = 20$ K.) of the dust, which is difficult to constrain with infrared emission, has been found from ISO and JCMT/SCUBA sub-mm observations (See Chapter 6.). Estimates of dust content are unfortunately biased by the dust temperature which is dominated by the illumination of the dust by stars and hampered by uncertainties in dust emissivity. In contrast, the extinction by dust is indicative of the total dust content of a spiral disk. Recently, we have proposed to characterize the opacity of the disks of M101 and M51 based on the number of distant galaxies seen through the disk. By comparing the extinction to other measurements of the interstellar medium we intend to learn more on the role of dust in the disk of spiral

galaxies.

The extinction in a foreground disk can be characterized once a known background source is identified. The rare pairs of occulting galaxies have been used to characterize absorption (White et al. (2000); Domingue et al. (2000); Keel and White (2001a,b)). A more generally applicable method is to use the number of distant galaxies seen through the disk of a spiral as the background source. González et al. (1998) used these and calibrated their number for the crowding and confusion using the “Synthetic Field Method”. Chapter 3 (Holwerda et al. 2005b) showed that both techniques agree well on disk extinction and presented radial extinction plots based on the counts of distant galaxies.

The new ACS data sets will bring down the uncertainties in the SFM opacity measurements as these provide a large solid angle on a *single* galaxy. In order to obtain the statistics for an opacity measurement, it is no longer necessary to combine several disks. Any systematics resulting from combining several different disks can now be avoided altogether.

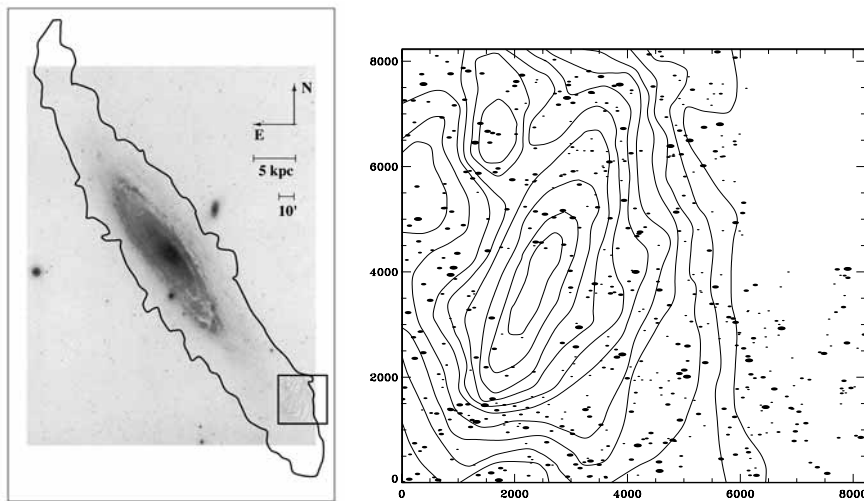


Figure 8.1: **Left:** A sketch of the field observed by Cuillandre et al. (2001) (square box at lower right) to the optical image of M31 (Sandage and Tammann (1981)). The thick contour is the large-scale H I emission extending over 5° (thick contour; at 8×10^{19} atoms cm^{-2}). **Right:** the distribution of large bright background galaxies over the image as identified from a visual inspection. The largest symbol corresponds to galaxies with $M_V = 18.5$. The remaining four smaller symbols indicate galaxy magnitudes ranging from 19 ± 0.5 (larger symbol) to 22 ± 0.5 mag (smallest symbol). The thin HI contours are drawn at levels of 2-18 in steps of 2, plus contours at 13 and 19, in units of 7.7×10^{19} atoms cm^{-2} from (Newton and Emerson (1977)). At higher HI column densities, there appear to be fewer galaxies. However, a much better comparison can be made using the many more galaxies that can be identified in HST images.

Figure 3.2 shows the radial extinction plot, averaged over several galaxies, based on counts of distant galaxies in HST/WFPC2 fields. The position of these fields was such, however, that the extinction measurements at higher radii ($R > R_{25}$) become much more

Table 8.1: M101 ACS Archival Fields

Field	Prop I.D.	Exp Time	(sec.)	
Nr		F814W	F555W	F435W
1- 9	9490	720	750	900
10-16	9492	360	360	360

uncertain. By analysing a large field on a single galaxy, we are confident an accurate measurement of the extent of the extinction in a disk can be made.

Cuillandre et al. (2001) analysed a field in M31, based on observations from the ground (Figure 8.1). They found a hint of an inverse relation between the numbers of bright galaxies they could identify and the HI column density. Using HST, the numbers of identifiable galaxies is greatly improved and a more direct comparison between HI column density and opacity can be made.

The emission from dust is being well characterized by the Spitzer Space Telescope. The three mid-infrared bands can map the position and temperature of the warm dust grains ($T \approx 40\text{-}60$ K.). By comparing this map to the extinction, a colder component can be inferred. In the case of M101, this would be the only way to detect this colder dust as sub-mm observations over such a large field would suffer too much from sky systematics.

Using the M51 and M101 mosaics, the following science questions can be addressed: to what radius does the extinction extend? Is there a cold dust component in the disk and how prominent is it? Is there a relation between the opacity of disks and their atomic hydrogen column density?

8.2 ACS data

There is Hubble Archival data on M101 and M51 that would be extremely suitable for analysis using the ‘‘Synthetic Field Method’’. Such large uniform data-sets could be used to test a fully automatic object-classification, using Self-Organising Maps. Fortunately, the method does not hinge on the success of this classification scheme as there is a semi-automated method, presented in Chapter 2 (Holwerda et al. 2005a).

8.2.1 M101

In cycle 11, proposals 9490 and 9492 resulted in HST imaging of most of M101’s disk. Originally these proposals were to identify optical counterparts for ultra-luminous x-ray sources (Kuntz and Chandra/HST M101 Collaboration (2004); Mukai et al. (2004)), to study the young starcluster population and to study HII regions in the outer disk. The position of the ACS fields are displayed in Figure 8.2. The two projects have three bands in common, the F814W (I), the F555W (V) and F435W (B) bands (See Table 1 for exposure times.). A mosaic of all 16 fields is shown in Figure 8.2. This is largest solid angle covered by HST on one single galaxy to date. This is approximately 1.5 times the solid angle of all the WFPC2 fields analysed in the previous chapters.

M101 is an ideal candidate to probe the extinction using distant galaxies. It is face-on and nearby enough to cover a large solid angle while distant enough to ease the granularity problems that plague counting efforts in nearby galaxies (See also Chapter 7). In addition,

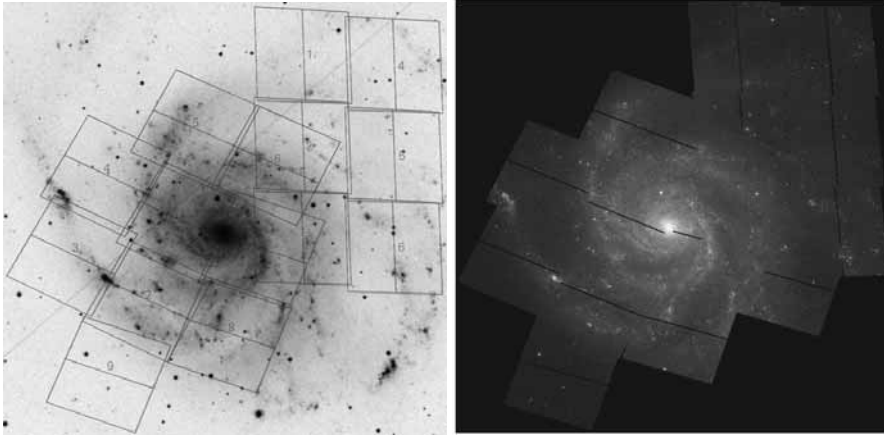


Figure 8.2: The mosaic of ACS pointings in M101. **Left:** The central-west set of 10 ACS pointings is from the 9490 proposal on ULX optical counterparts and stellar clusters and the 6 north-eastern are from the 9092 proposal to study HII regions. **Right:** The mosaic of ACS pointings in M101 (courtesy of the P.I. of proposal no. 9490, Dr. K. D. Kuntz). The visual check of ULX sources has already resulted in the identification of several background galaxies.

Table 8.2: The Heritage Program Observations

Filter	Individual Exp. Time (sec.)	Total Exp. Time (sec.)	Limiting Magnitude (mag)
B (F435W)	680	2720	27.3
V (F555W)	340	1360	26.5
I (F814W)	340	1360	25.8
H α (F658N)	680	2720	-

it has been well studied: a HI column density map is available and Spitzer imaging will be available from the archive in the near future.

This data has many advantages over the WFPC2 data used in the analysis by Holwerda et al. (2005a,b) and the ground based data in Cuillandre et al. (2001). A single-orbit ACS observation provides similar sampling and depth as a drizzled WFPC2 field but more importantly, a factor 3 improvement in field-of-view. The small pixel-size and photometric accuracy of the ACS will aid the identification process of objects in these fields. In addition, there are the two available colors (B-V and V-I) to help to identify objects.

Our initial estimate is that there are about 200,000 objects in this mosaic. This unique dataset with such a large number of uniformly imaged objects, opens the possibility to use a fully automated classification scheme.

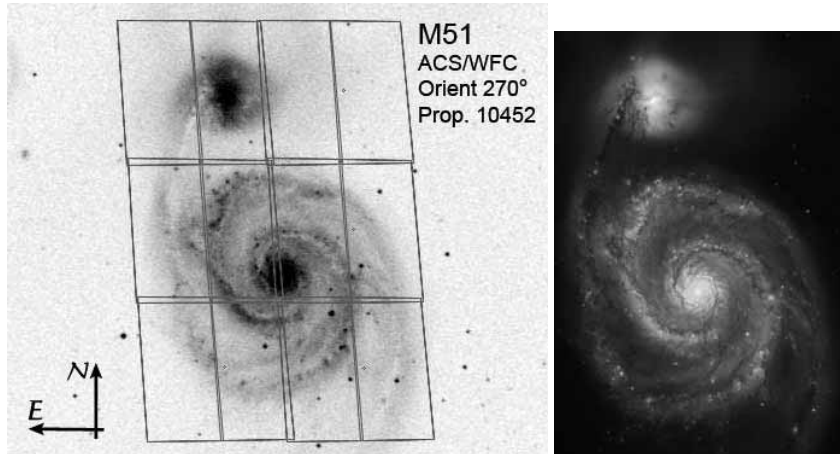


Figure 8.3: **Left:** The mosaic of ACS pointings for the Heritage proposal. Taken from <http://www.stsci.edu/hst/proposing/M51-heritage>. **Right:** The resulting mosaic. Table 8.2 lists the exposure times and expected limiting depths.

8.2.2 M51

The Hubble Heritage Team has announced deep, high-resolution imaging of M51 using the Advanced Camera for Surveys on board the Hubble Space Telescope in three photometric bands and a narrow $H\alpha$ filter (See Figure 8.3 and Table 8.2). These will be publicly available in April 2005 (proposal number 10452). Comparison fields are available from the GOODS survey and the Hubble Ultra Deep Field.

The observing strategy and choice of target is ideal for application of the SFM. M51 is face-on, at the right distance, and well studied for comparison. The observations span enough radial coverage and solid angle to reduce uncertainties in the estimates of average extinction. For example, one could compare the coverage by the ACS mosaic in Figure 8.3 to the two WFPC2 fields in Figure 8.4. The difference in solid angle covered is an order of magnitude, vastly improving statistics. The dithering strategy will not only cover the chip-gaps but also improve the sampling. This improvement in sampling should aid the identification process of distant galaxies at the distance of 8.4 Mpc.² The multiple exposures combine to a very deep imaging of disk of M51. While González et al. (1998) argued that the exposure time is not the limiting factor for the SFM, the high photometric precision from the high exposure times will, however, aid the determination of structural parameters such as asymmetry and concentration which can be used for object classifications. In addition, the three photometric bands will aid greatly in the identification process of objects in these fields. The fields in the narrow $H\alpha$ band can be used to identify the HII regions to safeguard against their selection as distant galaxies. Given the high quality of this data, we expect the identification process to be much less laborious than the earlier SFM work.

²See for a discussion on disk granularity, distance and resolution and how they affect distant galaxy detection, González et al. (2003) and Chapter 7 of this thesis (Holwerda et al. 2005e).

8.2.3 Object classification: the Self-Organizing Map

Automated classification of astronomical objects is a field on its own between computer science and astronomy. Star/galaxy separation, galaxy classification and spectral classification all have seen applications of neural networks. As long as there is a parameter space in which object classes are represented as sufficiently separate vectors, a neural network can perform classification as well as a human observer. The principle drawback of neural nets is that for each specific parameter-space and set of classes, a sufficiently sized training set needs to be supplied to train it.

Unsupervised neural networks however group the objects based on similarity and afterwards these groups can be classified, eliminating the need for a trainingset. An example of such an unsupervised network is the Kohonen Self-Organising Map (SOM, Kohonen (2001)). The SOM is a two dimensional field of "nodes", vectors of the same dimension as the vectors representing the astronomical objects. After the self organizing process, each object class correspond to a cluster of nodes on the map.

To train the SOM, each of the nodes is seeded with random values. The training algorithm then runs through the entire set of objects to be classified. Each object is compared to all the nodes on the map and the node most similar to the object is subsequently adjusted to resemble the object more. In addition, the neighbouring nodes in the map next to the winning node are adjusted as well, albeit not as much. This operation is repeated for a great number of objects and the measure of node adjustment is slowly damped. This causes the nodes in the map start to resemble the typical object vector for a certain class. Then only the object class associated with each node or cluster of nodes needs to be identified visually.

Self Organising Maps are a variant of unsupervised Neural Networks (NNW). The prerequisites for a successful classification with a SOM are that (1) the dataset is sufficiently large and spans all types of objects, (2) the parameter space chosen can differentiate between object classes. The classification itself requires a judicious choice of parameters (to maximize differentiation) and size of the map. Analogous to the size of parameterspace and the number of nodes (mapsize) would be the resolving power of a telescope's optics and the sampling of its point spread function (psf) by the detector.

We plan to find the right configuration of mapsize and parameterspace to classify the objects in the M101 and M51 catalogs and identify the background galaxies in the catalogs of science field and synthetic fields.

8.3 Disk opacity mapping

Once the background galaxies are identified in the science and synthetic fields of M101 and M51, their numbers can be compared to a series of characteristics of the disk: e.g. distance from the center, HI column density, surface brightness or infrared emission.

The projected distance from the galaxy center can be computed for each object in the catalogs, of both science and synthetic fields. The ratio between the number of synthetic and science galaxies as a function of radius can tell us the extent of the dust disk of M101 and M51. Earlier radial plots based on the numbers of distant galaxies were averaged over several galaxies (Chapter 3, Figure 3.2, Holwerda et al. (2005b)). To do so, the counts from several galaxies needed to be combined and coverage at higher radii was not optimal. This has the disadvantages that the radii had to be scaled and the radial coverage did not extend beyond the R_{25} (de Vaucouleurs et al. 1991) such that the

errors were small enough to determine accurately the radius at which there is no more extinction. Using the ACS data, a similar radial extinction plot can be constructed for only a single galaxy. The radius to which the extinction extends can then be much better determined as these fields extend to much greater distance from the center (Figures 8.2 and 8.3).

In addition, it becomes possible to compare the numbers of galaxies as a function of HI column density instead of radius. Thomas et al. (2004) present the possibility of a relation between HI emission and cold dust detected with SCUBA emission. In Chapter 4 the radial profiles were compared for individual galaxies. But instead of comparing HI and opacity per radial interval, a direct comparison would reveal any relation much better. With only two foreground galaxies, the number of distant galaxies can be directly compared per HI contour. Similar work was done on M31 by Cuillandre et al. (2001). Unfortunately, only the brightest galaxies can be identified in ground based data but their number does seem to drop with HI column density (Figure 8.1). The HI column densities can be obtained from the map from Kamphuis (1993) for M101 and Rots et al. (1990) for M51, both kindly provided by J.M. van der Hulst. The solid angle covered by the ACS mosaics are smaller than the field in Figure 8.1, but the accuracy and depth of the ACS fields will allow identification of many more distant background objects allowing for a much more accurate extinction measurement. Diffuse extinction and HI have been found to correlate in our own Galaxy. However, the absorption in a spiral disk as a whole is likely also due to dark clouds and these may anti-correlate with HI column density.

Meijerink et al. (2005) present a sub-millimeter map of M51. They find evidence of a cold extended dust disk. However, the sky background of the SCUBA scan map remains an unknown. The detection by SCUBA of extended emission therefore remains difficult. To compare, we plotted the opacity measurements from the two WFPC2 fields analysed as well (Figure 4.4). The uncertainties due to lack of solid angle make the comparison problematic although they *appear* to agree with the SCUBA result. If this is the case, the SCUBA emission and the extinction probe the same cold part of the ISM in the disk of M51. A radial plot from the ACS fields will have significantly reduced uncertainties as well as an extended radial coverage.

Stevens et al. (2005) assert that there are two components of dust, a warm (40-60 K) and a colder one (10-20K) in the spiral disk, based on infrared and sub-mm emission. The map of M51 by the Spitzer Space Telescope in the infrared can be used to track the warm component (Figure 8.4). The extinction traces the combination of both components. The comparison between the opacity map and the infrared emission should reveal the existence and relative import of the colder component.

The Spitzer Space Telescope has an approved program to obtain scan maps of all of M101 using both cameras on board, the IRAC and MIPS (GTO proposal no. 60, PI: George Rieke). By comparing the emission from dust grains from the MIPS images (at 24, 70 and 160 micron) to the extinction by dust, the existence and relative prominence of a colder component of the dust can be probed. A SCUBA measurement of the cold dust component of M101 is likely to be troubled by the sky component over such a large solid angle. However, SCUBA-2 might be able to do so. The difference between extinction and mid-infrared emission is likely the only way for a cold dust component to be found in M101.

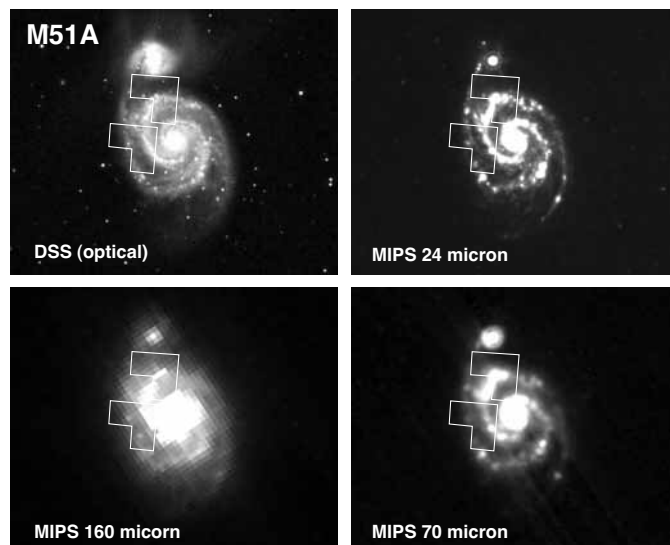


Figure 8.4: The Digital Sky Survey image and the three MIPS bands (24, 70 and 160 micron) with the two WFPC2 fields overlaid.

M101 is a spiral disk for which detailed metallicity gradients have been published (Kennicutt and Garnett (1996); Kennicutt et al. (2003b)). One could compare the dust gradient directly to this without the necessity to take the temperature gradient of the dust -as with emission- into account.

8.4 Concluding remarks

The counts of distant galaxies in archival HST/ACS data of M101 and M51 can address a series of scientific questions, often in combination with other existing data. The following questions can be answered: how far out beyond the optical disk do dust clouds extend? How does extinction and atomic hydrogen (HI) relate to each other in a spiral disk? How does the emission from dust -both sub-mm and infrared-, compare to the extinction? Is there a significant cold component of the dust in the disk? Is this cold dust extending beyond the optical disk? Does the metallicity and the dust content drop off with radius in a similar way?

With the wealth of comparison data and the high quality data-products, the above questions can be successfully addressed using this unique but proven observational technique.